Chapter 14

# Nonlinear Optics of Plasmonic Systems

## 14.1 Introduction to Plasmonics

In the present chapter we explore the optical properties of plasmonic systems. The word plasmonics is often associated with the properties of metals. The reason for this association is that both the electrical and optical properties of metals are intimately related to the large number of nearly free electrons present in the conduction band of a metal. In this chapter we will primarily be concerned with the optical properties of metals, although the fundamental results that we obtain equally well describe the optical properties of other types of plasmas. The properties of nearly free electrons have been described earlier in this book, for instance as a limiting case of the Lorentz model described in Section 1.4 and also in terms of relativistic effects of plasmas as described in Section 13.7. The present chapter seeks to describe the properties of plasmonic systems in a cohesive manner. Part of the reason for interest in plasmonic systems is that they display very strong light-matter coupling, and this strong coupling leads to both linear and nonlinear properties that can be qualitatively different from those of nonplasmonic systems. This coupling leads for example to a propagating wave, known as a surface plasmon polariton (SPP), which is a mixed excitation of both electron and electromagnetic field oscillations. Plasmonic systems also tend to display large nonlinear optical effects, both because metals often possess a large value of $\chi^{(3)}$ and because for the case of composite systems electric fields tend to become enhanced in regions near a metallic particle. More detailed accounts of the the role of plasmonics in nonlinear optics can be found in the accounts of Kauranen and Zayats (2012), Maier (2007), and Novotny and Hecht (2006a).

## 14.2 Simple Derivation of the Plasma Frequency

The concept of a plasma frequency is central to the understanding of plasmonic systems. The plasma frequency is the fundamental resonance frequency of a collection of free electrons.

**Nonlinear Optics.** https://doi.org/10.1016/B978-0-12-811002-7.00023-0

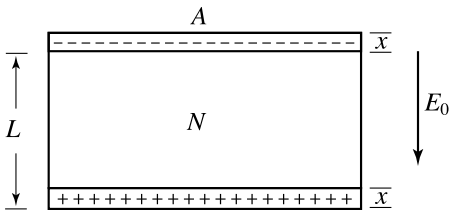


FIGURE 14.2.1: A static electric field $E_0$ is applied to a slab of metallic material of free charge density $N$.

Moreover, the expression for the plasma frequency appears in many of the equations that describe a plasmonic system.

In order to derive a mathematical expression for the plasma frequency, we consider a thin metallic slab of thickness $L$ and cross sectional area $A$ containing $N$ free electrons per unit volume, as shown in Fig. 14.2.1. A static electric field of strength $E_0$ is initially applied to this structure, which pulls the electrons upward leaving a region of positive charge at the bottom of the structure. At time $t = 0$ the static field is suddenly switched off, and we wish to determine the subsequent motion of the charge distribution.

As a simple model, we assume that the electron distribution moves as a rigid object. We let $x$ denote the distance through which the electron distribution has been displaced from its equilibrium position. The total electric charge contained in the region at the top of the slab is thus given by $Q = -NeAx$. Similarly, the total charge in the region at the bottom of the slab is given by $NeAx$. Under the reasonable assumption of $x \ll L$, we can describe each of these distributions in terms of a surface charge density (that is, charge per unit area) given by

$$\sigma_{\text{top}} = -Nex \equiv -\sigma, \tag{14.2.1}$$

$$\sigma_{\text{bottom}} = Nex. \tag{14.2.2}$$

Each of these charge distributions gives rise to an electric field of magnitude $\sigma/(2\epsilon_0)$ arranged as shown in parts (a) and (b) of Fig. 14.2.2, as can be readily verified through use of Gauss's law. The total field in the region between the two charge distributions is thus given by the superposition of these field contributions, that is, by

$$E_{\text{tot}} = \frac{\sigma}{\epsilon_0} = \frac{Nex}{\epsilon_0} \tag{14.2.3}$$

as shown in part (c) of the figure.

We now require that the collection of electrons located at the top of the stab, considered as a rigid body, satisfies Newton's second law in the form $F = M\ddot{x}$, where the force $F$ is given by

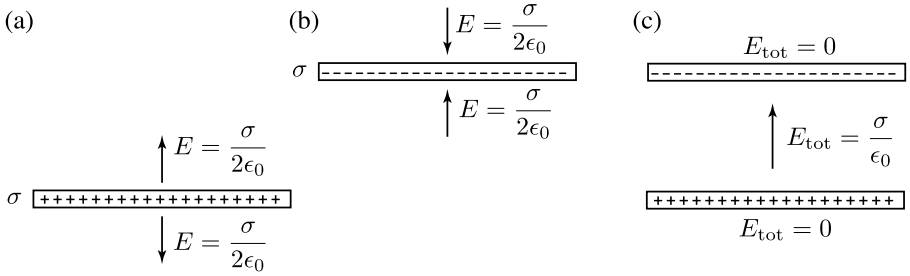


FIGURE 14.2.2: The unbalanced charge at the bottom (a) and top (b) of the slab creates fields of magnitude $\sigma/(2\epsilon_0)$ oriented as shown. By the linear superposition principle, the total field is given by $\sigma/\epsilon_0$ within the slab and vanishes elsewhere (c).

$QE_{\rm tot}$, where as above $Q = -NeAx$. Also, the total mass of these electrons is $M = NmAx$, where $m$ is the mass of the electron. We thus find that

$$\frac{-Ne^2x}{\epsilon_0 m} = \ddot{x}, \tag{14.2.4}$$

which has the solution

$$x(t) = x_0 e^{-i\omega_p t} + \text{c.c.}, \tag{14.2.5}$$

where

$$\omega_p = \sqrt{\frac{Ne^2}{\epsilon_0 m}} \tag{14.2.6}$$

is known as the plasma frequency. It is the characteristic frequency at which a collection of free electrons oscillates. This equation gives the standard result for the plasma frequency. It can be generalized in several ways. For example, for the case of a conducting solid the electron mass $m$ can be replaced by the effective mass $m^*$ to take account of the band structure of the material. Moreover, if the metallic slab is characterized by a relative dielectric permittivity $\epsilon$, then the expression for the plasma frequency becomes

$$\omega_p = \sqrt{\frac{Ne^2}{\epsilon\epsilon_0 m^*}}. \tag{14.2.7}$$

## 14.3 The Drude Model

We next present a simple model that describes the optical properties of a metal or other plasmonic system. The model treats the metal as a gas of free electrons. The model is related to

the Lorentz model described elsewhere in this book by assuming that the restoring force and thus the resonance frequency $\omega_0$ vanishes. In fact, many of the results of this section can be obtained by taking the limit of $\omega_0 \to 0$ of the Lorentz model. However, we will instead derive the relevant equations here in order to make the present section self contained. For now, we will treat only the linear response, and will treat nonlinear behavior in the following sections.

We consider the motion of a free electron exposed to a laser field of the form

$$\tilde{E}(t) = E_0 e^{-i\omega t} + \text{c.c.} \tag{14.3.1}$$

We consider the force on the electron to be of the form

$$\tilde{F}(t) = -e\tilde{E}(t) - 2m\gamma\dot{\tilde{x}} \tag{14.3.2}$$

where $\gamma$ represents a damping constant and where the dot denotes a time derivative. The equation of motion $\tilde{F}(t) = m\ddot{\tilde{x}}$ thus becomes

$$\ddot{\tilde{x}} + 2\gamma\dot{\tilde{x}} = -e\tilde{E}(t)/m \tag{14.3.3}$$

which has the solution

$$\tilde{x}(t) = x_0 e^{-i\omega t} + \text{c.c.} \quad \text{where} \quad x_0 = \frac{eE_0/m}{\omega^2 + 2i\omega\gamma}. \tag{14.3.4}$$

We next determine the susceptibility in the standard manner. We take the polarization amplitude to be $P(\omega) = -ex_0$ and introduce the linear susceptibility through the relation $P = \epsilon_0 \chi^{(1)} E_0$ and thus find that

$$\chi^{(1)} = -\frac{Ne^2/(m\epsilon_0)}{\omega^2 + 2i\omega\gamma} = -\frac{\omega_p^2}{\omega^2 + 2i\omega\gamma} \tag{14.3.5}$$

where in obtaining the last form we have introduced the plasma frequency of Eq. (14.2.6). We now use the standard result $\epsilon^{(1)}(\omega) = 1 + \chi^{(1)}(\omega)$ to obtain

$$\epsilon^{(1)}(\omega) = 1 - \frac{\omega_p^2}{\omega^2 + 2i\omega\gamma}. \tag{14.3.6}$$

This equation gives the standard Drude result. It can be expressed in terms of its real and imaginary parts as

$$\epsilon^{(1)}(\omega) = \left[1 - \frac{\omega_p^2}{\omega^2 + 4\gamma^2}\right] + i\left[\frac{2\omega_p^2\gamma}{\omega(\omega^2 + 4\gamma^2)}\right]. \tag{14.3.7}$$

Note that in the limit $\omega \to 0$ the real part of $\epsilon^{(1)}(\omega)$ approaches the value $1 - \omega_p^2/4\gamma^2$ whereas the imaginary part diverges. These functional dependences are plotted in Fig. 14.3.1 for the representative case in which $\gamma/\omega_0$ is equal to 0.05.

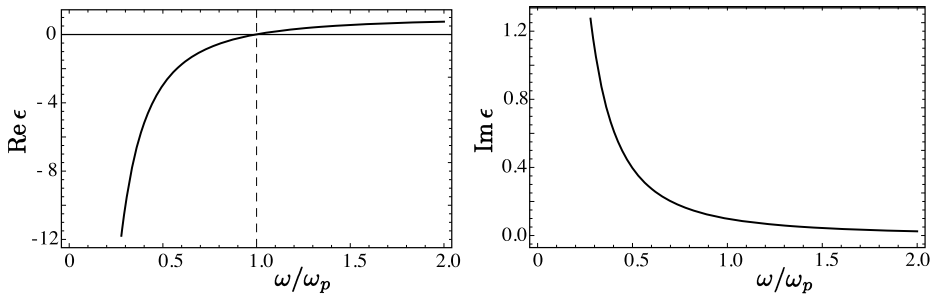


FIGURE 14.3.1: The frequency dependence of the real and imaginary parts of the dielectric permittivity $\epsilon(\omega)$ according to the Drude model.

For the special case in which loss is negligible and we can let $\gamma$ approach zero in Eq. (14.3.6), we can find a very simple expression for the dispersion relation (that is, the relation between $k$ and $\omega$) for a free-electron gas. We note that $k = n\omega/c$ and thus that $k^2 = \epsilon^{(1)}(\omega)\omega^2/c^2$. We then take $\epsilon^{(1)}(\omega)$ to be equal to $1 - \omega_p^2/\omega^2$ and find that

$$k^2c^2 = \omega^2 - \omega_p^2. \tag{14.3.8}$$

We see that the propagation constant $k$ can be a real quantity, which is the case for a propagating wave, only for $\omega > \omega_p^2$. Light at frequencies smaller than $\omega_p^2$ cannot propagate through a gas of free electrons. If a wave is incident from a dielectric onto such a medium, it will be totally reflected.

The standard Drude result of Eq. (14.3.6) can be generalized in several ways. For example, the "1" in this equation can be replaced by $\epsilon_\infty$ to obtain

$$\epsilon^{(1)}(\omega) = \epsilon_\infty - \frac{\omega_p^2}{\omega^2 - 2i\omega\gamma}. \tag{14.3.9}$$

Here the first term $\epsilon_\infty$ represents the nonresonant contribution of bound electrons, whereas the second term represents the contribution of free electrons. A different generalization is to take explicit account of the contributions of the bound electrons by adding to the right-hand side of this last equation a Lorentz-like contribution so that it becomes

$$\epsilon^{(1)}(\omega) = \epsilon_\infty - \frac{\omega_p^2}{\omega^2 - 2i\omega\gamma} + \frac{N_b e^2/(\epsilon_0 m)}{\omega_0^2 - \omega^2 - 2i\omega\gamma_b}. \tag{14.3.10}$$

In this equation $N_b$ is the number density of bound electrons, $\omega_0$ is the resonance frequency, and $\gamma_b$ is the damping coefficient for the bound electrons.

More refined models for the response of free electrons to an electromagnetic field can be obtained through use of the hydrodynamic model. Here the electrons are treated as comprising an isotropic gas such that the electron velocity field $\mathbf{v}$ is required to obey the equation

$$mN\left[\frac{\partial \mathbf{v}}{\partial t} + (\mathbf{v}\cdot\nabla)\mathbf{v} + \frac{\mathbf{v}}{\tau}\right] = -eN(\mathbf{E} + \mathbf{v}\times\mathbf{B}) - \nabla p, \tag{14.3.11}$$

where $m$ is the effective electron mass, $N$ is the number density, $\tau$ is the electron damping time, and $p$ is any pressure including quantum pressure (Sipe et al., 1980).

## 14.4 Optical Properties of Gold

In this section we review some of the linear and nonlinear optical properties of gold. We concentrate on gold because it is widely used in studies of plasmonics. Gold is classified as a noble metal, that is, a metal that is resistant to corrosion in air. Its chemical stability is only one reason for its choice as a preferred material for use in plasmonics. In addition, the number density $5.90 \times 10^{28}$ m$^{-3}$ of free electrons in gold is large, thus leading to strong light-plasma interactions.

The optical properties of gold are well known. Fig. 14.4.1 displays the measured dielectric function $\epsilon^{(1)}(\omega)$ of gold along with two models of the frequency dependence of $\epsilon^{(1)}$. The measured values are taken from the well-known study of Johnson and Christy (1972). We see that the Drude model of Eq. (14.3.6) provides a very good fit to the data for frequencies lower than approximately $3 \times 10^{15}$ rad/sec. The Drude model fails at higher frequencies because it accounts only for the free-electron response. A better fit is obtained by adding a Lorentz-oscillator contribution to the dielectric response. This fit, based on the use of Eq. (14.3.10) provides a good fit to the data for frequencies up to $4 \times 10^{15}$ rad/sec. A good fit at higher frequencies could be obtained by including more resonance frequencies in the model.

These optical properties can be understood in terms of the electronic structure of gold. The (nearly filled) valence band is comprised of 5d electrons, and the approximately half-filled conduction band is comprised of 6sp electrons. This band is referred to as the 6sp band as it is believed that it has both s-like and p-like character. The electrons in the conduction band can be considered to be essentially free electrons, and lead to a plasma frequency $\omega_p$ of $1.28 \times 10^{16}$ rad/sec. This frequency corresponds to a vacuum wavelength of 147 nm. Light of wavelength shorter than approximately 500 nm can induce transitions from the valence band to the conduction band. This absorption of blue light leads to the "gold" color of gold.

The nonlinear optical properties of gold are dominated by three primary mechanisms (Hache et al., 1988; Boyd et al., 2014).

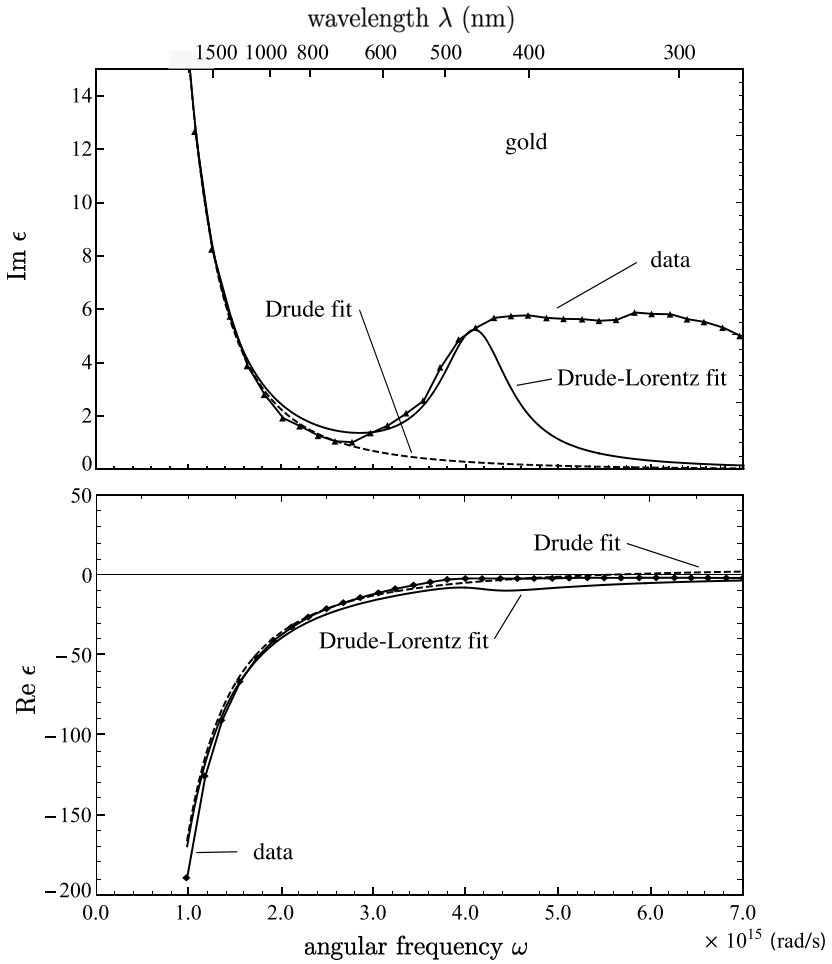


FIGURE 14.4.1: The frequency dependence of the real and imaginary parts of the dielectric permittivity $\epsilon(\omega)$ of gold. The curve labeled data gives the results of Johnson and Christy (1972). The curve labeled Drude gives a good fit to the data for frequencies up to $3 \times 10^{15}$ rad/sec. The curve labeled Drude–Lorentz includes the influence of one resonance frequency and fits the data up to a frequency of $4 \times 10^{15}$ rad/sec. A good fit could be obtained at higher frequencies by including more resonance frequencies into the model. The Drude-model fit makes use of the parameters $\epsilon_\infty = 6$, $\omega_p = 1.28 \times 10^{16}$ rad/sec corresponding to a wavelength of 147 nm, and $\Gamma = 1.25 \times 10^{14}$ s$^{-1}$. The Drude–Lorentz fit makes use of the parameters $\epsilon_\infty = 1$, $\omega_0 = 4.19 \times 10^{15}$ rad/sec, and $\Gamma = 9 \times 10^{14}$ s$^{-1}$.

The first mechanism is the contribution of the "free" electrons in the conduction band. Of course, this contribution would vanish (in the electric dipole approximation that we consider here) for electrons that are entirely free of any restoring force, for the simple reason that if there is no restoring force there can be no nonlinearity in this force. However, when these electrons

are confined within a nanoparticle, they display nonlinear optical effects. These effects can be modeled by performing a "particle-in-a-box" calculation. Hache et al. have performed such a calculation and find that a typical value of the third-order susceptibility is $10^{-18}$ m$^2$/V$^2$.

The second mechanism is interband transitions between the conduction and valence bands. The nonlinear response can be understood as saturation of this absorption process. For light at the resonance frequency, this contribution can be considered to produce a primarily imaginary contribution to $\chi^{(3)}$. Hache et al. estimate this contribution to be of the order of $2.4i \times 10^{-16}$ m$^2$/V$^2$.

The third mechanism is what is known as the hot-electron contribution. This contribution involves electrons that are laser-excited from the 5d valence band to the 6sp conduction band. The energy carried by this excitation process ends up heating the electrons in the conduction band. The change in temperature of the conduction-band electrons modifies the Fermi–Dirac distribution function, leading to an increased population for energies above the Fermi level and a decrease in population for energies below the Fermi level. As a result, the dielectric function of gold is changed in a strongly frequency-dependent manner. Because of the mechanism just described, the hot-electron contribution is often alternatively referred to as the Fermi-smearing contribution. A typical value of the resulting third-order susceptibility $\chi^{(3)}$ is $1.4i \times 10^{-16}$ m$^2$/V$^2$. Detailed experimental studies of the response time of the hot-electron contribution have been reported by Sun et al. (1994). These authors find that the nonlinear response is not instantaneous but is associated with a turn-on time of approximately 500 fs. This value is determined by the time taken for the energy carried by the excitation process to thermalize and heat the conduction electrons. Furthermore, the nonlinear response decays with a relaxation time of several picoseconds. This is the time required for the temperature of the electrons to equilibrate with that of the lattice. Since the heat capacity of the lattice is much larger than that of the electrons, the hot-electron contribution essentially vanishes once this equilibration has occurred. Because of the noninstantaneous nature of the nonlinear optical response, the measured value of $\chi^{(3)}$ is found to be strongly dependent on laser pulse duration. The dependence has been analyzed by Boyd et al. (2014).

## 14.5 Surface Plasmon Polaritons

We next turn to the discussion of surface plasmon polariton (SPP). An SPP is an electromagnetic disturbance that is fundamentally distinct from those that we have studied elsewhere in this book. An SPP travels along the interface between two different materials, typically a metal and a dielectric. The name polariton refers to a disturbance that entails the coupling of an electromagnetic wave with a material excitation; in this particular case the material excitation is a plasma oscillation.

To describe the SPP mathematically, we consider the situation shown in Fig. 14.5.1. Here the plane $z = 0$ separates two materials of dielectric permittivity $\epsilon_m$ and $\epsilon_d$. For definiteness,

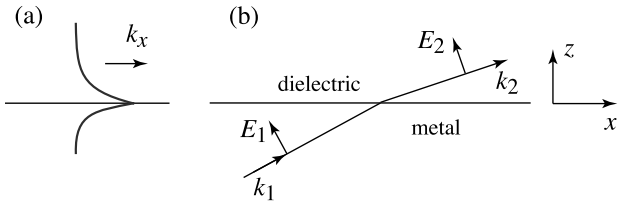


FIGURE 14.5.1: (a) Symbolic representation of an SPP propagating in the $z$ direction along the interface between a metal and a dielectric. (b) Geometry and definition of quantities involved in the determination of the dispersion relation for the propagation of an SPP.

we assume that $\epsilon_m$ is complex and that $\epsilon_d$ is real. We seek a solution of Maxwell's equation that describes a wave propagates in the $x$ direction along the interface and that is localized in the $z$ direction near the interface at $z = 0$. We assume the wave to be p-polarized, that is, polarized in the plane of the diagram. We represent the electric field of the light wave to be of the form

$$\tilde{\mathbf{E}}_{\mathrm{m}}(\mathbf{r}, t) = \left(A_{\mathrm{m},x}\hat{x} + A_{\mathrm{m},z}\,\hat{z}\right) e^{i(k_x x - \omega t)} e^{ik_{\mathrm{m},z} z} \tag{14.5.1}$$

for $z < 0$ and of the form

$$\tilde{\mathbf{E}}_{\mathrm{d}}(\mathbf{r}, t) = \left(A_{\mathrm{d},x}\hat{x} + A_{\mathrm{d},z}\,\hat{z}\right) e^{i(k_x x - \omega t)} e^{ik_{\mathrm{d},z} z} \tag{14.5.2}$$

for $z > 0$. Note that we have assumed that the waves have the same propagation constant $k_x$ for propagation in the $x$ direction, but we allow them to have different spatial dependences in the $z$ direction. We seek solutions for which both $k_{\mathrm{m},z}$ and $k_{\mathrm{d},z}$ have imaginary components, which allows the wave to be localized near the interface.

We next examine how the four field amplitudes $A_{\mathrm{m},x}$, $A_{\mathrm{m},z}$, $A_{\mathrm{d},x}$, and $A_{\mathrm{d},z}$ are related to one another. The Maxwell equation $\nabla \cdot \tilde{\mathbf{D}} = 0$ applied to a monochromatic plane wave implies that $\mathbf{k} \cdot \tilde{\mathbf{D}} = 0$ and thus that $k_x D_{j,x} + k_{j,z} D_{j,z} = 0$ for $j = \mathrm{m}, \mathrm{d}$. Since $\tilde{\mathbf{D}}_j = \epsilon_j \tilde{\mathbf{E}}_j$, we find that $k_x \epsilon_j E_{j,x} + k_{j,z} \epsilon_j E_{j,z} = 0$ and thus that $k_x \epsilon_j A_{j,x} + k_{j,z} \epsilon_j A_{j,z} = 0$ and finally that

$$\begin{aligned} k_x A_{\mathrm{m},x} + k_{\mathrm{m},z} A_{\mathrm{m},z} &= 0, \\ k_x A_{\mathrm{d},x} + k_{\mathrm{d},z} A_{\mathrm{d},z} &= 0. \end{aligned} \tag{14.5.3}$$

Other relations between the four field amplitudes arise from the boundary conditions at the interface. The requirement that the components of the electric field $\tilde{\mathbf{E}}$ along the interface must be continuous leads to the relation

$$A_{\mathrm{m},x} - A_{\mathrm{d},x} = 0. \tag{14.5.4}$$

Moreover, the requirement that the components of the $\tilde{\mathbf{D}}$ field normal to the interface be continuous leads to the relation

$$\epsilon_{\mathrm{m}} A_{\mathrm{m},x} - \epsilon_{\mathrm{d}} A_{\mathrm{d},x} = 0. \tag{14.5.5}$$

These equations ((14.5.3), (14.5.4), and (14.5.5)) constitute a set of four homogeneous equations in four unknowns. They can readily be written in the form of a matrix equation, and the condition for the existence of a nonvanishing solution is that the determinant of the matrix of coefficients must vanish. This condition leads to the characteristic equation

$$k_x(k_{\mathrm{d},z}\epsilon_{\mathrm{m}} - k_{\mathrm{m},z}\epsilon_{\mathrm{d}}) = 0. \tag{14.5.6}$$

This equation possesses two solutions. The solution $k_x = 0$ does not correspond to an excitation propagating along the interface and is not the solution of interest to us. The other solution, which corresponds to a wave propagating along the interface in the $x$ direction, is given by

$$k_{\mathrm{d},z}\epsilon_{\mathrm{m}} - k_{\mathrm{m},z}\epsilon_{\mathrm{d}} = 0. \tag{14.5.7}$$

To find the form of the electromagnetic wave corresponding to this solution, we also require that Eqs. (14.5.1) and (14.5.2) each obey a wave equation of the form $\nabla^2\mathbf{E} - (\boldsymbol{\epsilon}/c^2)\cdot(\partial^2\mathbf{E}/\partial t^2) = 0$ (see also Eq. (2.1.21)). This requirement leads to the equations

$$k_x^2 + k_{\mathrm{m},z}^2 = \epsilon_{\mathrm{m}}(\omega^2/c^2) \tag{14.5.8}$$

and

$$k_x^2 + k_{\mathrm{d},z}^2 = \epsilon_{\mathrm{d}}(\omega^2/c^2). \tag{14.5.9}$$

Eqs. (14.5.7), (14.5.8), and (14.5.9) can now be solved simultaneously to find that

$$k_x^2 = \frac{\omega^2}{c^2}\frac{\epsilon_{\mathrm{m}}\epsilon_{\mathrm{d}}}{\epsilon_{\mathrm{m}} + \epsilon_{\mathrm{d}}} \quad \text{or that} \quad k_x = \frac{\omega}{c}\sqrt{\frac{\epsilon_{\mathrm{m}}\epsilon_{\mathrm{d}}}{\epsilon_{\mathrm{m}} + \epsilon_{\mathrm{d}}}}. \tag{14.5.10}$$

This equation provides the dispersion relation for an SPP, that is, it tells how the longitudinal component of the wavevector is related to the optical frequency. This dependence is displayed graphically in Fig. 14.5.2.

One similarly finds that the component of the propagation vector perpendicular to the interface is given in each of the two media by

$$k_{\mathrm{m},z} = k\sqrt{\frac{\epsilon_{\mathrm{m}}^2}{\epsilon_{\mathrm{m}} + \epsilon_{\mathrm{d}}}} \quad \text{and} \quad k_{\mathrm{d},z} = k\sqrt{\frac{\epsilon_{\mathrm{d}}^2}{\epsilon_{\mathrm{m}} + \epsilon_{\mathrm{d}}}}. \tag{14.5.11}$$

We next interpret these results. We are seeking a solution that propagates in the $x$ direction, and we thus require $k_x$ of Eq. (14.5.10) to be a real quantity. We thus see that $\epsilon_{\mathrm{m}}\epsilon_{\mathrm{d}}$ and $\epsilon_{\mathrm{m}} + \epsilon_{\mathrm{d}}$ must both have the same sign. We also require that both $k_{\mathrm{m},z}$ and $k_{\mathrm{d},z}$ possess an imaginary component so that they can describe a wave that decays exponentially aways from the interface in both the positive and negative $z$ directions. From the second of Eqs. (14.5.11) we see that $\epsilon_{\mathrm{m}} + \epsilon_{\mathrm{d}}$ must be negative, and thus by the first condition we see that the product $\epsilon_{\mathrm{m}}\epsilon_{\mathrm{d}}$ must also

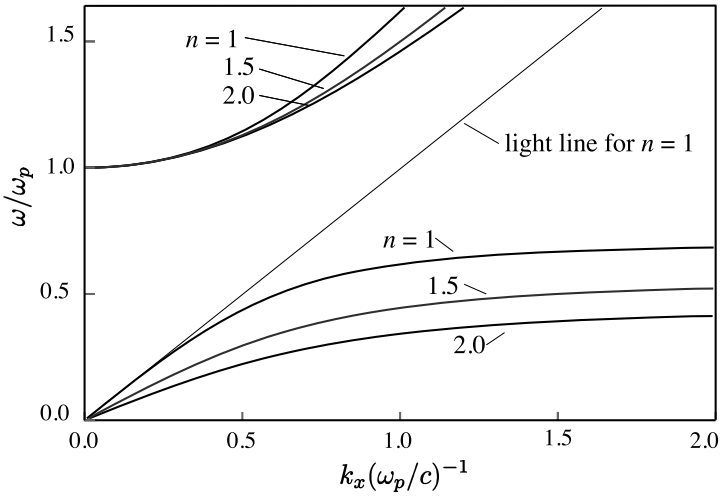


FIGURE 14.5.2: Plot of the dispersion relation for an SPP (Eq. (14.5.10)) at the interface between a dielectric of various refractive indices a metal modeled by the lossless Drude model (Eq. (14.3.6)). Note that the asymptotic value for large $k_x$ of the lower branch is given by $\omega_p/\sqrt{\epsilon_d + 1)}$.

be negative. Thus $\epsilon_m$ and $\epsilon_d$ must have opposite signs. Also, to satisfy the condition that $\epsilon_m + \epsilon_d$ be negative, we require that the absolute value of the negative quantity, which we identify with $\epsilon_m$, must be larger than $\epsilon_d$. We have seen in Fig. 14.3.1 that metals can show a large, negative value of $\epsilon_m$. We anticipated these conclusions by calling one the materials the metal and calling the other material the dielectric.

The propagation of SPPs show pronounced nonlinear effects. This result is to be expected, because metals tend to be highly nonlinear and because for an SPP there is strong field confinement at the interface. De Leon et al. (2014) have investigated nonlinear behavior for SPPs on a gold–air interface. The report an intensity-dependent contribution to the propagation constant $k_x$ given by

$$\Delta k_x = \gamma_{sp} S_{sp} \tag{14.5.12}$$

where $S_{sp}$ in units of power per unit length (W/m) is a measure of the intensity of the laser excitation in the one-transverse-dimension geometry of a surface excitation and $\gamma_{sp}$ in units of $W^{-1}$ is the nonlinear coefficient of the SPP. These authors report a value of $\gamma_{sp} = (8.08 + i1.46) \times 10^{-7}\ W^{-1}$.

## 14.6 Electric Field Enhancement in Plasmonic Systems

The interplay of metals and dielectrics can lead to strong resonant behavior, leading to strong light-matter coupling and consequently to large linear and nonlinear optical effects. This strong

light-matter coupling can most simply be understood as originating in the lightning-rod effect. There is a strong enhancement of the local electric field in the vicinity of a sharp point or tip. This strong field enhancement can lead to strong nonlinear optical effects, a well known example of which is surface enhanced Raman scattering (Moskovits, 2005; Kneipp et al., 1996). It is also the basis of near-field optical microscopy. Moreover, it can lead to enhancement of the nonlinear optical response (Smith et al., 1997; Grésillon et al., 1999).

It is difficult to obtain analytic solutions to Maxwell's equations for highly pointed objects of the sort mentioned in the last paragraph. Instead, we will turn to a different model, that of a dielectric or metal sphere placed in an otherwise uniform electric field. We will find that this simple model gives us an opportunity to understand many of the feature of field enhancement in plasmonic systems.

We consider a metallic* sphere of radius $a$ and complex dielectric constant $\epsilon_m$ placed in a background material of dielectric constant $\epsilon_b$, as shown in Fig. 14.6.1. A uniform (except for the disturbance caused by the metal particle) electric field of strength $E_0$ fills the interaction region. We assume that the wavelength $\lambda$ of this radiation is much larger than the particle size $a$, and thus we can treat this problem as if the applied field were static; this approximation for $a << \lambda$ is known as the quasistatic approximation.

This situation is a well-known problem in electrostatics, and we will simply quote the standard result (Stratton, 2007; Jackson, 1999; Maier, 2007). One finds that the field inside the sphere is spatially uniform and is given by

$$E_{in} = \frac{3\epsilon_b}{\epsilon_m + 2\epsilon_b} E_0. \tag{14.6.1}$$

The sphere thus acquires a dipole moment that can be expressed as

$$p = \epsilon_0 \epsilon_m \alpha E_0 \tag{14.6.2}$$

where the polarizability of the sphere is given by

$$\alpha = 4\pi a^3 \frac{3\epsilon_b}{\epsilon_m + 2\epsilon_b}. \tag{14.6.3}$$

The field outside the sphere is given by the sum of $E_0$ and the well-known expression for the field of a dipole. The field in the neighborhood of the dipole is shown in Fig. 14.6.1.

The nature of electric field enhancement in plasmonics can be understood by studying Eq. (14.6.1), which relates the field $E_{in}$ inside the sphere to the incident field $E_0$. The coefficient $[3\epsilon_b/(\epsilon_m + 2\epsilon_b)]$ can be understood as the local field enhancement factor for this situation. We recall (see for instance Fig. 14.4.1) that metals possess a negative dielectric function that

* We will continue to call this particle a metal sphere, although the following analysis hold equally well for a dielectric particle.

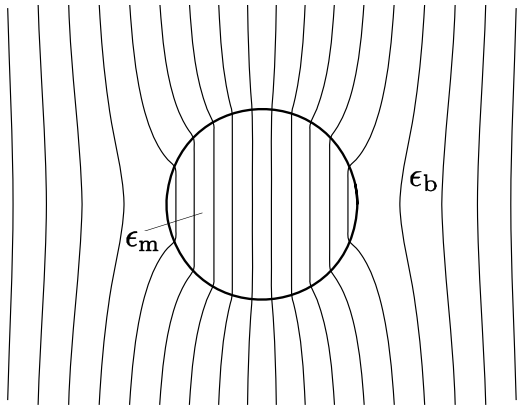


FIGURE 14.6.1: Electric field distribution in the neighborhood of a polarizable sphere placed in an otherwise uniform electric field. The situation $\epsilon_m = 2$ and $\epsilon_b = 1$ is shown. Note that the electric field is drawn in towards the region of the sphere.

is strongly frequency dependent. Under many circumstances the real part of the denominator of the local field factor vanishes at some particular frequency, leading to a large enhancement in the local field. This situation is known as the Fröhlich condition, and leads to the surface plasmon resonance. For real materials, the local field factor $[3\epsilon_b/(\epsilon_m + 2\epsilon_b)]$ can be as large as 30.

## Problems

1. In Section 14.5 we assumed that the radiation incident upon the interface was p-polarized, and we found solutions to Maxwell's equations in the form of a surface plasmon polariton (SPP). Do SPPs occur for s-polarization?
2. We noted that Eq. (14.5.6) possesses the solution $k_x = 0$. Determine the form of the electromagnetic disturbance associated with this solution.

## References

Plasma Frequency and Drude Model

Kauranen, M., Zayats, A.V., 2012. Nat. Photonics 6, 737.

Maier, S.A., 2007. Plasmonics: Fundamentals and Applications. Springer.

Novotny, L., Hecht, B., 2006a. Principles of Nano-Optics, 2nd Edition. Cambridge University Press.

Sipe, J.E., So, V.C.Y., Fukui, M., Stegeman, G.I., 1980. Phys. Rev. B 21, 4389.

### Optical Properties of Gold

Boyd, R.W., Shi, Z., De Leon, I., 2014. Opt. Commun. 326, 7479.
Hache, F., Ricard, D., Flytzanis, C., Kreibig, U., 1988. Appl. Phys. A 47, 347.
Johnson, P.B., Christy, R.W., 1972. Phys. Rev. B 6, 4370.
Sun, C.K., Vallee, F., Acioli, L.H., Ippen, E.P., Fujimoto, J.G., 1994. Phys. Rev. B 50, 15337.

### Surface Plasmon Polaritons

See also the analogous treatment of SPPs given by Novotny, L., Hecht, B., 2006b. Principles of Nano-Optics, 2nd Edition. Cambridge University Press.
De Leon, I., Shi, Z., Liapis, A.C., Boyd, R.W., 2014. Opt. Lett. 39, 2274.

### Electric Field Enhancement in Plasmonic Systems

Grésillon, S., Aigouy, L., Boccara, A.C., Rivoal, J.C., Quelin, X., Desmarest, C., Gadenne, P., Shubin, V.A., Sarychev, A.K., Shalaev, V.M., 1999. Phys. Rev. Lett. 82, 4520.
Jackson, J.D., 1999. Classical Electrodynamics, vol. 4, Third Edition. John Wiley & Sons, Section 4.4.
Kneipp, K., et al., 1996. Phys. Rev. Lett. 78, 1667.
Moskovits, M., 2005. J. Raman Spectrosc. 36, 485.
Smith, D.D., Fischer, G., Boyd, R.W., Gregory, D.A., 1997. J. Opt. Soc. Amer. B 14, 1625.
Stratton, J.A., 2007. Electromagnetic Theory. John Wiley & Sons.